

Modelling of H₂/D₂ exchange over Pd

H. Backman*, K. Rahkamaa-Tolonen, J. Wärnä, T. Salmi, D. Yu. Murzin

Laboratory of Industrial Chemistry, Process Chemistry Centre, Åbo Akademi, FIN-20500 Turku/Åbo, Finland

Abstract

The isotopic exchange between hydrogen and deuterium was studied over a Pd/alumina catalyst. A model was proposed, including the adsorption and dissociation of hydrogen and deuterium. An adsorption-assisted desorption mechanism was also included and turned out to play a minor role in the H₂/D₂ exchange but have to be considered in the reaction between deuterium and water. A comparison between the experimental data and the simulation revealed that the model could describe the observed dissociation and isotope exchange reaction.

© 2004 Elsevier B.V. All rights reserved.

Keywords: Isotopic exchange; Mechanism; Kinetic modelling

1. Introduction

The interaction of hydrogen with metal surfaces is a fundamental problem of surface science. Because of its apparent simplicity, the investigation of hydrogen adsorption on metal surfaces has regained experimental interest with respect to both the dissociation behaviour and the atomic adsorption properties. In environmental catalysis, the main issue is to optimise catalytic converters to remove pollutants. A detailed understanding of the kinetic processes taking place simultaneously and interactively is therefore needed. Transient response methods offer several advantages for investigation of the kinetics of heterogeneous catalytic reactions. Tamaru and Naito [1], Mirodatos [2], and Furusawa et al. [3] have reviewed the transient technique applied to heterogeneous catalysis. The system can be perturbed in a controlled way by changing any system variable such as concentration, temperature, flow rate, or pressure. While undergoing a dynamic change the system reveals more about the mechanism, compared to steady-state experiments. A more specific way to use the transient techniques is the steady-state isotopic transient kinetic analysis. This involves replacement of a reactant by its isotopically labelled counterpart in the form of a step or pulse input function. The thermodynamic state of the system remains constant in the experiment and the reaction kinetics

may be assessed close to a steady state. Isotope-labelled reactants are therefore used to follow reaction pathways and to determine reaction mechanism, compared to steady-state experiments. The kinetic analysis of transient response data is based on nonlinear regression analysis. Equations are established for each and every gas phase and surface species which results in a set of coupled differential equations [4]. The isotopic transient techniques have been widely used to develop new technologies in the field of environmental catalysis [5,6]. It has also been applied in the linear modelling of catalytic surface reactions [7] and in mathematical treatments of transient kinetic data [4]. In the present work, deuterium step changes have been utilised to trace the hydrogen reaction pathways over Pd–alumina, as it eventually can help in developing a fundamental understanding of the role of hydrogen in the reduction of NO.

2. Experimental

The isotopic exchange between hydrogen and deuterium was studied using isotopic changes between 1% H₂/Ar and 1% D₂/Ar over a Pd/alumina catalyst in a quartz reactor having a length of 300 mm and a diameter of approximately 8 mm. The catalyst used in the experimental section was a modified alumina-supported Pd catalyst. The active metal, palladium, was attached to the support by means of impregnation using Pd/(NO₃)₂ as a precursor. The metal content in the washcoat was 1.06%. The BET surface area determined

* Corresponding author. Tel.: +358 2 2154479; fax: +358 2 2154479.

E-mail addresses: hbackman@abo.fi (H. Backman), dmurzin@abo.fi (D. Yu. Murzin).

Nomenclature

c	concentration vector, gas-phase components
c*	concentration vector, surface intermediate
M	stoichiometric matrix, surface intermediates
N	stoichiometric matrix, gas-phase intermediates
P	total pressure
r	rate vector, gas-phase components
r*	rate vector, surface components
R	rate vector, elementary steps
R	gas constant
R²	degree of explanation
t	time
T	temperature
V	volume
\dot{V}	volumetric flow rate
x	molar fraction vector
z	dimensionless length coordinate

Greek letters

δ	dimensionless change in the volumetric flow rate
ε	void fraction
θ	fractional coverage vector
Θ	dimensionless time
ρ	catalyst bulk density
σ	specific surface area of the catalyst
τ	contact time

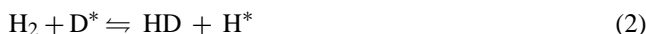
by nitrogen adsorption was 112 m²/g and the pore volume of the catalyst was 0.33 cm³/g. The palladium particle size determined by CO chemisorption was approximately 3.2 nm. The total gas flow over the catalyst was 400 ml/min and the reaction temperature 155 ± 3 °C. The experiments were carried out under atmospheric pressure. A split of the product flow was taken through a capillary to a quadrupole mass spec-

trometer. Experiments with D₂ and H₂O were also performed to determine the deuterium exchange with hydrogen in water. The details about the analytical and experimental procedure have been reported by Rahkamaa-Tolonen et al. [8].

3. Results and reaction mechanism

In the present study, hydrogen was initially pre-adsorbed on the surface. Once deuterium was introduced to the reactor the isotopic exchange took place with the hydrogen atoms already adsorbed, and formation of HD was immediately observed. At this point the formation of HD started to grow until a maximum, after which it decreased in a short period of time. The reverse process could be observed when deuterium flow was switched off and hydrogen flow introduced into the reactor. This can also be seen in Fig. 1. Production of water was observed in the first and last step of the experiment, which can be attributed to the reaction of chemisorbed H* -atoms and OH-groups present in the alumina support. Small amounts of HDO and D₂O could be observed during the second stage of the experiment.

Based on the transient responses and literature data, two different mechanisms were proposed for the isotopic exchange reaction, H₂/D₂. The first mechanism, denoted as mechanism A, is assuming exchange between atomic hydrogen/deuterium and a molecule [9]:



When more vacant sites are available, D₂ dissociates and reacts further with the H* atoms according to the following reactions [10]:

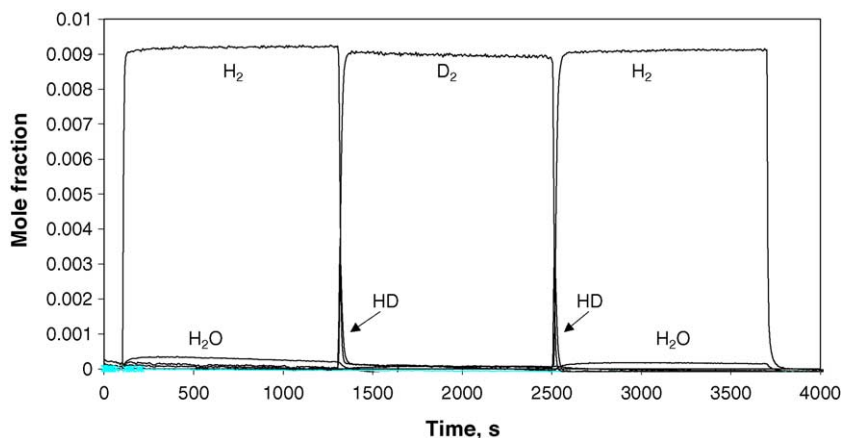


Fig. 1. H₂/D₂ exchange over Pd/alumina at 155 °C.

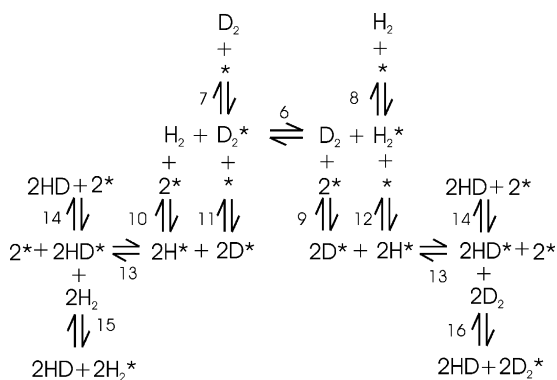


Fig. 2. Mechanism B for the H₂/D₂ exchange over Pd.

The second mechanism illustrated in Fig. 2, assuming adsorption-assisted desorption with molecular hydrogen/deuterium is denoted as mechanism B. D₂ molecules interact with adsorbed hydrogen atoms and enhances their association and desorption. Tamaru and Naito [1] first proposed the adsorption-assisted-desorption concept and many authors have later largely reviewed it.

To clarify the reaction mechanism for the isotope exchange between water and deuterium experiments were performed with H₂O and D₂, over the same catalyst and under the same condition as the H₂/D₂ experiment. Once water entered the reactor dissociation took place and the isotopic products HDO, D₂O and HD started to form (Fig. 3). The H* atoms were assisted to desorb from the surface by D₂ molecules simultaneously arriving to the catalyst. The formation of the H₂ peak can be attributed to the adsorption-assisted desorption mechanism. No deuterium response was observed in the beginning of the experiment indicating adsorption and dissociation of deuterium. Rahkamaa-Tolonen et al. [8] proposed based upon the observations a model for the formation of hydrogen as follows:

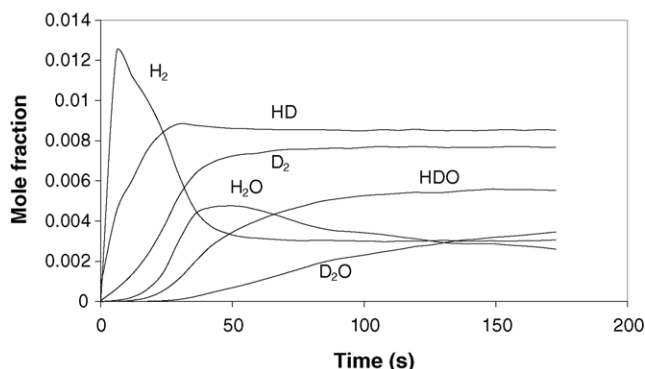
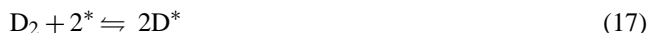
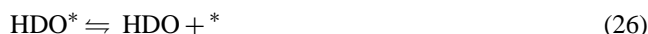


Fig. 3. H₂/D₂ isotopic exchange in H₂O over Pd at 155 °C.



4. Mathematical method

Like all kinetic modelling, the kinetic modelling of the H₂/D₂ exchange requires experimental data with sufficient information content to allow verification of reaction mechanism and meaningful parameter estimation. Usually the case is that kinetic models for catalytic reactions contain a large number of parameters, which requires high experimental accuracy. The kinetic analysis of a reaction can be performed with the use of model fitting and nonlinear regression analysis. This allows testing of alternative reaction mechanisms since commonly the case is that several models could be fitted to the same reaction. A challenge in kinetic analysis is hence to distinguish a unique functional form of the kinetic model. Transient techniques provide in general better mechanism identifiability than steady-state experiments.

The parameter estimation and modelling of the reactions in this work is based on the data of the gas phase combined with the theoretical calculations of the coverages for the surface intermediates. The transient step-responses were described quantitatively with a dynamic plug flow model where adsorption, surface reaction, and desorption steps were included. Two mechanistic models for the H₂/D₂ exchange were tested taking into account the adsorption and dissociation of hydrogen including an adsorption-assisted desorption mechanism. The first comprises steps (1)–(5) and the second is depicted in Fig. 2. The gas-phase components and surface intermediates were described with separate mass balances. The kinetic parameters were determined with nonlinear regression analysis.

The isothermal plug flow model for the components in the gas phase is written as

$$\frac{dc}{dt} = -\varepsilon^{-1} \frac{d(c\dot{V})}{dV} + \sigma\rho_B\varepsilon^{-1}\mathbf{r} \quad (29)$$

Defining the dimensionless quantities and replacing the concentrations by mole fractions, the mass balance can be written in dimensionless form

$$\frac{d\mathbf{x}}{d\Theta} = -\varepsilon^{-1} \left(\delta \frac{d\mathbf{x}}{dz} + \mathbf{x} \frac{d\delta}{dz} \right) + \frac{\sigma\rho_B\tau RT_0}{\varepsilon P_0} \mathbf{NR} \quad (30)$$

The rates of the elementary steps are given by vector \mathbf{R} and the generation rates of gas phase (\mathbf{r}) and surface components (\mathbf{r}^*) are calculated from

$$\mathbf{r} = \mathbf{NR} \quad (31)$$

$$\mathbf{r}^* = \frac{d\mathbf{c}^*}{dt} = \mathbf{MR} \quad (32)$$

where \mathbf{N} and \mathbf{M} denote the stoichiometric matrices for the gas phase and surface components [11].

Instead of using surface concentration surface coverage (θ_j), calculated from $\mathbf{c}^* = \theta_j c_0$ where c_0 is the total concentration of active sites can be used. When dimensionless time is inserted the final form of the balance becomes

$$\frac{d\theta}{d\Theta} = \left(\frac{\tau}{c_0} \right) \mathbf{MR} \quad (33)$$

The initial conditions of the gas phase and surface balance equations are

$$\mathbf{x} = \mathbf{x}_0(z) \quad (34)$$

$$\theta = \theta_0(z), \quad \Theta < 0, \quad 0 \leq z \leq 1 \quad (35)$$

The rates of the elementary steps for the H_2/D_2 exchange explained by reaction mechanism A are given by the following equations:

$$\begin{aligned} R_{\text{H}_2} &= -r_2 + r_{-2} - r_3 + r_{-3}, \\ R_{\text{D}^*} &= r_1 - r_{-1} - r_2 + r_{-2} + 2r_4 - 2r_{-4} - r_5 \\ R_{\text{HD}} &= r_1 - r_{-1} + r_2 - r_{-2} + r_5, \\ R_{\text{H}^*} &= -r_1 + r_{-1} + r_2 - r_{-2} + 2r_3 - 2r_{-3} - r_5 \\ R_{\text{D}_2} &= -r_1 + r_{-1} - r_4 + r_{-4}, \\ R_* &= -(R_{\text{D}^*} + R_{\text{H}^*}) \end{aligned}$$

where the single steps are:

$$\begin{aligned} r_1 &= k_1 \cdot c_{\text{D}_2} \cdot c_{\text{H}^*}, & r_{-1} &= k_{-1} \cdot c_{\text{D}^*} \cdot c_{\text{HD}} \\ r_2 &= k_2 \cdot c_{\text{H}_2} \cdot c_{\text{D}^*}, & r_{-2} &= k_{-2} \cdot c_{\text{H}^*} \cdot c_{\text{HD}} \\ r_3 &= k_3 \cdot c_{\text{H}_2} \cdot c_*^2, & r_{-3} &= k_{-3} \cdot c_{\text{H}^*}^2 \\ r_4 &= k_4 \cdot c_{\text{D}_2} \cdot c_*^2, & r_{-4} &= k_{-4} \cdot c_{\text{D}^*}^2 \\ r_5 &= k_5 \cdot c_{\text{D}^*} \cdot c_{\text{H}^*}, \end{aligned}$$

The concentration is denoted by c , k the rate constant and c_{A^*} the concentration of the adsorbed species A, etc.

The rates of the elementary steps for mechanism B, based on Fig. 2, are:

$$\begin{aligned} R_{\text{H}_2} &= -r_6 + r_{-6} - r_8 + r_{-8} - r_{10} + r_{-10} - r_{15} + r_{-15}, & R_* &= -r_7 + r_{-7} - r_8 + r_{-8} - 2r_9 + 2r_{-9} - 2r_{10} + 2r_{-10} - r_{11} \\ & & & + r_{-11} - r_{12} + r_{-12} + r_{13} - r_{-13} + r_{14} - r_{-14} \\ R_{\text{HD}} &= r_{14} - r_{-14} + r_{15} - r_{-15} + r_{16} - r_{-16}, & R_{\text{H}^*} &= 2r_{10} - 2r_{-10} + 2r_{12} - 2r_{-12} - r_{13} + r_{-13} \\ R_{\text{D}_2} &= r_6 - r_{-6} - r_7 + r_{-7} - r_9 + r_{-9} - r_{16} + r_{-16}, & R_{\text{D}^*} &= 2r_9 - 2r_{-9} + 2r_{11} - 2r_{-11} - r_{13} + r_{-13} \\ & & & R_{\text{H}_2^*} = r_6 - r_{-6} + r_8 - r_{-8} - r_{12} + r_{-12} + r_{15} - r_{-15} \\ & & & R_{\text{D}_2^*} = -r_6 + r_{-6} + r_7 - r_{-7} - r_{11} + r_{-11} + r_{16} - r_{-16} \\ & & & R_{\text{HD}^*} = r_{13} - r_{-13} - r_{14} + r_{-14} - r_{15} + r_{-15} - r_{16} + r_{-16} \end{aligned}$$

where the single steps are:

$$\begin{aligned} r_6 &= k_6 \cdot c_{\text{D}_2^*} \cdot c_{\text{H}_2}, & r_{-6} &= k_{-6} \cdot c_{\text{D}_2} \cdot c_{\text{H}_2^*} \\ r_7 &= k_7 \cdot c_{\text{D}_2} \cdot c_*, & r_{-7} &= k_{-7} \cdot c_{\text{D}_2^*} \\ r_8 &= k_8 \cdot c_{\text{H}_2} \cdot c_*, & r_{-8} &= k_{-8} \cdot c_{\text{H}_2^*} \\ r_9 &= k_9 \cdot c_{\text{D}_2} \cdot c_*^2, & r_{-9} &= k_{-9} \cdot c_{\text{D}^*}^2 \\ r_{10} &= k_{10} \cdot c_{\text{H}_2} \cdot c_*^2, & r_{-10} &= k_{-10} \cdot c_{\text{H}^*}^2 \\ r_{11} &= k_{11} \cdot c_{\text{D}_2^*} \cdot c_*, & r_{-11} &= k_{-11} \cdot c_{\text{D}^*}^2 \\ r_{12} &= k_{12} \cdot c_{\text{H}_2^*} \cdot c_*, & r_{-12} &= k_{-12} \cdot c_{\text{H}^*}^2 \\ r_{13} &= k_{13} \cdot c_{\text{D}^*} \cdot c_{\text{H}^*}, & r_{-13} &= k_{-13} \cdot c_{\text{HD}^*} \cdot c_* \\ r_{14} &= k_{14} \cdot c_{\text{HD}^*}, & r_{-14} &= k_{-14} \cdot c_{\text{HD}} \cdot c_* \\ r_{15} &= k_{15} \cdot c_{\text{HD}^*} \cdot c_{\text{H}_2}, & r_{-15} &= k_{-15} \cdot c_{\text{H}_2^*} \cdot c_{\text{HD}} \\ r_{16} &= k_{16} \cdot c_{\text{HD}^*} \cdot c_{\text{D}_2}, & r_{-16} &= k_{-16} \cdot c_{\text{D}_2^*} \cdot c_{\text{HD}} \end{aligned}$$

The model predictions were obtained by solving the differential equations numerically for all of the components during the parameter estimation. The PDEs, Eq. (30), were converted to ODEs by the method of lines. The ODEs were solved with the ODE-solver (BzzOde) suitable for stiff differential equation was used to solve the system of equations with the backward difference method. The ODE-solver connected to a parameter-estimation program, MODEST [12], was used for the estimation of the kinetic parameters. The simplex algorithm implemented in the software minimized the residual sum of squares. The most common measure for the goodness of fit is the R^2 -value, given by the expression

$$R^2 = 100 \left(1 - \frac{\|c_{\text{exp}} - c_{\text{est}}\|^2}{\|c_{\text{exp}} - \bar{c}_{\text{exp}}\|^2} \right) \quad (36)$$

where the values c_{est} denote the predictions given by the model and \bar{c}_{exp} the mean value of all the data points.

For the $\text{D}_2 + \text{H}_2\text{O}$ reaction the elementary steps are given as follows.

For gas species:

$$\begin{aligned} R_{\text{H}_2} &= r_{21} - r_{-21} \\ R_{\text{HD}} &= r_{22} - r_{-22} + r_{24} - r_{-24} \\ R_{\text{D}_2} &= -r_{17} + r_{-17} - r_{21} + r_{-21} - r_{22} + r_{-22} \\ R_{\text{H}_2\text{O}} &= -r_{18} + r_{-18} \\ R_{\text{HDO}} &= r_{26} - r_{-26} \\ R_{\text{D}_2\text{O}} &= r_{28} - r_{-28} \end{aligned}$$

For surface species:

$$R_* = -2r_{17} + 2r_{-17} - r_{18} + r_{-18} - r_{19} + r_{-19} + r_{20} - r_{-20} + r_{23} - r_{-23} + r_{24} - r_{-24} + r_{25} - r_{-25} + r_{26} - r_{-26} + r_{28} - r_{-28}$$

$$R_{D^*} = 2r_{17} - 2r_{-17} - r_{23} + r_{-23} - r_{25} + r_{-25} - r_{27} + r_{-27}$$

$$R_{H_2O} = r_{18} - r_{-18} - r_{19} + r_{-19}$$

$$R_{H^*} = -2r_{20} + 2r_{-20} - r_{23} + r_{-23} + r_{27} - r_{-27}$$

$$R_{OH^*} = r_{19} - r_{-19} - r_{25} - r_{-25}$$

$$R_{H_2^*} = r_{20} - r_{-20} - r_{21} + r_{-21}$$

$$R_{D_2^*} = r_{21} - r_{-21} + r_{22} - r_{-22}$$

$$R_{HD^*} = -r_{22} + r_{-22} + r_{23} - r_{-23} - r_{24} + r_{-24}$$

$$R_{HDO^*} = r_{25} - r_{-25} - r_{26} + r_{-26} - r_{27} + r_{-27}$$

$$R_{D_2O^*} = r_{27} - r_{-27} - r_{28} + r_{-28}$$

and for the single steps the rates are:

$$\begin{aligned} r_{17} &= k_{17} \cdot c_{D_2} \cdot c_*^2, & r_{-17} &= k_{-17} \cdot c_{D^*}^2 \\ r_{18} &= k_{18} \cdot c_{H_2O} \cdot c_*, & r_{-18} &= k_{-18} \cdot c_{H_2O^*} \\ r_{19} &= k_{19} \cdot c_{H_2O^*} \cdot c_*, & r_{-19} &= k_{-19} \cdot c_{H^*} \cdot c_{OH^*} \\ r_{20} &= k_{20} \cdot c_{H^*}^2, & r_{-20} &= k_{-20} \cdot c_{H_2^*} \cdot c_* \\ r_{21} &= k_{21} \cdot c_{H_2^*} \cdot c_{D_2}, & r_{-21} &= k_{-21} \cdot c_{H_2} \cdot c_{D_2^*} \\ r_{22} &= k_{22} \cdot c_{HD^*} \cdot c_{D_2}, & r_{-22} &= k_{-22} \cdot c_{D_2^*} \cdot c_{HD} \\ r_{23} &= k_{23} \cdot c_{D^*} \cdot c_{H^*}, & r_{-23} &= k_{-23} \cdot c_{HD^*} \cdot c_* \\ r_{24} &= k_{24} \cdot c_{HD^*}, & r_{-24} &= k_{-24} \cdot c_{HD} \cdot c_* \\ r_{25} &= k_{25} \cdot c_{OH^*} \cdot c_{D^*}, & r_{-25} &= k_{-25} \cdot c_{HDO^*} \cdot c_* \\ r_{26} &= k_{26} \cdot c_{HDO^*}, & r_{-26} &= k_{-26} \cdot c_{HDO} \cdot c_* \\ r_{27} &= k_{27} \cdot c_{HDO^*} \cdot c_{D^*}, & r_{-27} &= k_{-27} \cdot c_{D_2O^*} \cdot c_{H^*} \\ r_{28} &= k_{28} \cdot c_{D_2O^*}, & r_{-28} &= k_{-28} \cdot c_{D_2O} \cdot c_* \end{aligned}$$

5. Discussion

The two mechanisms for the H₂/D₂ exchange were tested separately. When all steps were considered in the parameter estimation for mechanism A, the values of the parameters for steps (1) and (2) were close to zero resulting in high standard errors for the parameters, as can be seen from Table 1. To test whether the adsorption-assisted desorption, e.g. steps (1) and (2), is significant for the reaction the rate constants for steps (1) and (2) were fixed to zero. This resulted in an improvement of the parameter errors but the degree of explanation decreased, which is presented in Table 2. For mechanism B, a similar observation was made. When all steps in the mechanism were included in the parameter estimation the values of the steps attributed to the molecular adsorption-assisted desorption, steps (6), (15) and (16), were found to be very low after optimum fit to the experimental data (Table 1). In this form, the mechanism could not describe the H₂/D₂ exchange sufficiently well, indicating that this parameter set represents

Table 1

Estimated values of the parameters for H₂/D₂ exchange, all steps included in the calculations

Mechanism A: all parameters (degree of explanation 99.41%)	
Parameter	Estimated values
k_1 (l/mol s)	$1.36 \times 10^{-3} \pm 5.13 \times 10^{-3}$
k_{-1} (l/mol s)	$5.38 \times 10^{-3} \pm 0.0143$
k_2 (l/mol s)	$6.79 \times 10^{-3} \pm 0.011$
k_{-2} (l/mol s)	$0.0134 \pm 2.69 \times 10^{-3}$
k_3 (l ² /mol ² s)	0.912 ± 0.12
k_{-3} (l/mol s)	0.0919 ± 0.0131
k_4 (l ² /mol ² s)	1.18 ± 0.124
k_{-4} (l/s)	0.124 ± 0.012
k_5 (l/mol s)	0.21 ± 0.0115
Mechanism B: all parameters (degree of explanation 96.69%)	
Parameter	Estimated values
k_6 (l/mol s)	$1.24 \times 10^{-5} \pm 7.58 \times 10^{-4}$
k_{-6} (l/mol s)	$2.41 \times 10^{-4} \pm 0.0196$
k_7 (l/mol s)	0.122 ± 0.129
k_{-7} (s ⁻¹)	0.033 ± 0.00596
k_8 (l/mol s)	0.49 ± 0.0277
k_{-8} (s ⁻¹)	$0.179 \pm 1.68 \times 10^{-4}$
k_9 (l ² /mol ² ·s)	6.44 ± 0.313
k_{-9} (l/mol s)	0.774 ± 0.0631
k_{10} (l ² /mol ² ·s)	5.15 ± 0.0907
k_{-10} (l/mol s)	0.595 ± 0.0551
k_{11} (l/mol s)	$1.15 \pm 2.24 \times 10^{-3}$
k_{-11} (l/mol s)	0.656 ± 0.0163
k_{12} (l/mol s)	0.21 ± 0.0288
k_{-12} (l/mol s)	0.531 ± 0.0434
k_{13} (l/mol s)	0.66 ± 5.21
k_{-13} (l/mol s)	0.253 ± 0.0202
k_{14} (s ⁻¹)	0.546 ± 0.00134
k_{-14} (l/mol s)	0.169 ± 0.012
k_{15} (l/mol s)	$4.63 \times 10^{-4} \pm 2.68 \times 10^{-3}$
k_{-15} (l/mol s)	$9.68 \times 10^{-4} \pm 7.97 \times 10^{-4}$
k_{16} (l/mol s)	$7.42 \times 10^{-4} \pm 1.76 \times 10^{-3}$
k_{-16} (l/mol s)	$6.25 \times 10^{-3} \pm 0.016$

probably a local, but not global, minimum. When the rate constants for the steps (6), (15) and (16) in mechanism B (Fig. 2) were set to zero, the mechanism was able to describe the isotopic exchange H₂/D₂ on Pd in the best way with a degree of explanation of 99.7%. As can be seen from Fig. 4, the comparison between experimental data and modelled simulations demonstrated successful modelling. The parameters and the statistics are presented in Table 2. The results reveal that dissociation of hydrogen and deuterium is the prevailing mechanism. This result is in agreement with previous experiments, which demonstrates that hydrogen is adsorbed dissociatively on palladium [13].

Modelling and parameter estimation for the D₂ + H₂O reaction was also performed. It was important to reveal if the adsorption-assisted desorption step proposed by Rahkamaa-Tolonen et al., step (21), was significant for the reaction mechanism. During the parameter estimation of this mechanism, the rate constant for step (21) was either included or excluded (rate constant equal to zero) from the calculations. If step (21) was included the degree of explanation (96.8%)

Table 2

Estimated values of the parameters for H₂/D₂ exchange, without adsorption assisted desorption

Mechanism A (degree of explanation 98.64%)	
Parameter	Estimated values
k_3 (l ² /mol ² s)	0.81 ± 0.134
k_{-3} (l/mol·s)	$0.08 \pm 8.68 \times 10^{-5}$
k_4 (l ² /mol ² s)	1.06 ± 0.0709 l ² /mol ² ·s
k_{-4} (s ⁻¹)	0.10 ± 0.015 1/s
k_5 (l/mol·s)	$0.06 \pm 4.37 \times 10^{-3}$ l/mol·s
Mechanism B (degree of explanation 99.7%)	
Parameter	Estimated
k_7 (l/mol s)	0.019 ± 0.016 l/mol·s
k_{-7} (s ⁻¹)	0.011 ± 0.012 1/s
k_8 (l/mol s)	0.018 ± 0.018 l/mol·s
k_{-8} (s ⁻¹)	0.024 ± 0.019 1/s
k_9 (l ² /mol ² s)	11 ± 5.27 l ² /mol ² ·s
k_{-9} (l/mol s)	1.33 ± 0.61 l/mol·s
k_{10} (l ² /mol ² s)	8.35 ± 0.09
k_{-10} (l/mol s)	10.4 ± 0.122 l/mol·s
k_{11} (l/mol s)	3.4 ± 0.24 l/mol·s
k_{-11} (l/mol s)	1.9 ± 0.17 l/mol·s
k_{12} (l/mol s)	2.54 ± 0.57 l/mol·s
k_{-12} (l/mol s)	2.14 ± 1.25 l/mol·s
k_{13} (l/mol s)	0.66 ± 0.45 l/mol·s
k_{-13} (l/mol s)	$1.8 \times 10^{-3} \pm 2.45 \times 10^{-4}$ l/mol·s
k_{14} (s ⁻¹)	$0.67 \pm 2.75 \times 10^{-4}$ 1/s
k_{-14} (l/mol s)	0.19 ± 0.11

as well as the estimated parameter errors was acceptable. Without taking step (21) into account the degree of explanation remained below 80%. This could lead to the conclusion that adsorption-assisted desorption plays a minor role in the H₂/D₂ exchange but have to be considered in the reaction between deuterium and water. The hydrogen peak immediately after the introduction of D₂ and H₂O can clearly be assigned to the adsorption-assisted desorption phenomena, in which deuterium interacts with chemisorbed H* in order to liberate active sites and then dissociate. Fig. 5 displays the compari-

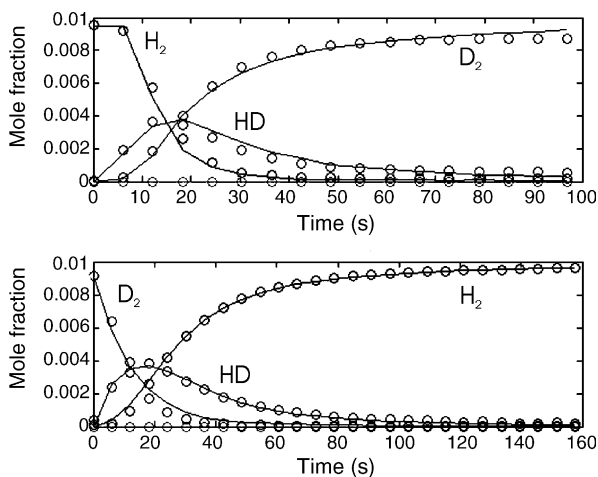


Fig. 4. H₂/D₂ exchange on Pd/alumina. Comparison between experimental data (symbols) and calculations (curves). The degree of explanation is 99.7%.

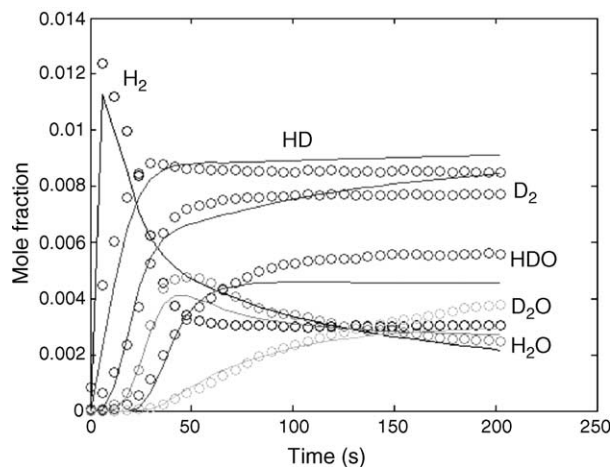


Fig. 5. D₂ + H₂O on Pd/alumina. Comparison between experimental data (symbols) and calculations (curves). Degree of explanation is 96.8%.

Table 3

Estimated parameters for the modelling of D₂ + H₂O reaction on Pd/alumina

Parameter	Estimated values
k_{17} (l ² /mol ² s)	4.92 ± 3.35
k_{-17} (l/mol s)	2.07 ± 2.23
k_{18} (l/mol s)	4.06 ± 2.24
k_{-18} (s ⁻¹)	1.34 ± 0.532
k_{19} (l/mol s)	0.653 ± 0.859
k_{-19} (l/mol s)	$2.85 \times 10^{-3} \pm 4.83 \times 10^{-4}$
k_{20} (l/mol s)	3.85 ± 4.62
k_{-20} (l/mol s)	$2.72 \times 10^{-3} \pm 1.6 \times 10^{-3}$
k_{21} (l/mol s)	$4.27 \times 10^{-3} \pm 1.23 \times 10^{-3}$
k_{-21} (l/mol s)	$4.24 \times 10^{-3} \pm 3.19 \times 10^{-3}$
k_{22} (l/mol s)	5.97 ± 1.7
k_{-22} (l/mol s)	$6.1 \times 10^{-3} \pm 1.7 \times 10^{-3}$
k_{23} (l/mol s)	2.88 ± 3.29
k_{-23} (l/mol s)	3.2 ± 2.84
k_{24} (s ⁻¹)	0.228 ± 0.07
k_{-24} (l/mol s)	0.0456 ± 0.0361
k_{25} (l/mol s)	1.58 ± 0.802
k_{-25} (l/mol s)	4.18 ± 2.11
k_{26} (s ⁻¹)	0.414 ± 0.58
k_{-26} (l/mol s)	4.83 ± 3.83
k_{27} (l/mol s)	0.525 ± 0.0918
k_{-27} (l/mol s)	1.42 ± 0.269
k_{28} (s ⁻¹)	0.102 ± 0.138
k_{-28} (l/mol s)	6.47 ± 8.63

son between experimental data and modelled simulations for the D₂ + H₂O reaction to the experimental data and the parameter statistics is summarized in Table 3. As can be seen, the proposed model is able to describe the transient behaviour of the system.

6. Conclusions

Kinetic modelling of the isotopic exchange between hydrogen and deuterium over Pd/Al₂O₃ was performed in this study by nonlinear regression. Based on experimental results, reaction mechanisms were developed for the H₂/D₂ exchange

as well as for the hydrogen/deuterium isotopic exchange in H₂O over Pd. Adsorption-assisted desorption had to be included in the mechanism for hydrogen/deuterium isotopic exchange in H₂O whereas H₂/D₂ exchange could be modelled without it.

References

- [1] K. Tamaru, S. Naito, in: G. Ertl, H. Knözinger, J. Weitkamp (Eds.), *Handbook of Heterogeneous Catalysis*, vol. 3, VCH, Weinheim, 1997.
- [2] C. Mirodatos, *Catal. Today* 9 (1991) 83–95.
- [3] T. Furusawa, M. Suzuki, J.M. Smith, *Catal. Rev.-Sci. Eng.* 13 (1976) 43–76.
- [4] S.C. van der Linde, T.A. Nijhuis, F.H.M. Dekker, F. Kapteijn, J.A. Moulijn, *Appl. Catal. A* 151 (1997) 27–57.
- [5] A.A. Shestov, R. Burch, J.A. Sullivan, *J. Catal.* 186 (1999) 362–372.
- [6] M.W. Kumthekar, U.S. Ozkan, *Appl. Catal. A* 151 (1997) 289–303.
- [7] S.L. Shannon, J.G. Goodwin, *Appl. Catal. A* 151 (1997) 3–26.
- [8] K. Rahkamaa-Tolonen, T. Salmi, D. Yu. Murzin, L. Barreto Dillon, H. Karhu, R. Keiski, L. Väyrynen, *J. Catal.* 210 (2002) 17–29.
- [9] B.M.W. Trapnell, *Catalysis: Hydrogenation and Dehydrogenation*, vol. 3, Reinhold Publishing Corporation, New York, 1955, pp. 1–48.
- [10] S.-I. Miyamoto, T. Sakka, M. Iwasaki, *Can. J. Chem.* 67 (1989) 857–861.
- [11] T. Salmi, *Comp. Chem. Eng.* 11 (1987) 83–94.
- [12] H. Haario, *Modest 6.0 – A User's Guide*, ProfMath, Helsinki, 2001.
- [13] E. Miyazaki, *J. Catal.* 65 (1980) 84–94.